JOURNAL OF MATERIALS SCIENCE 17 (1982) 2324–2336

Effects of notch length, specimen thickness, ply thickness and type of defect on the fracture behaviour of angle-ply graphite–epoxy composites

S. OCHIAI*, P. W. M. PETERS
DFVLR, Institut Für Werkstoff-Forschung, Postfach 90 60 58, 5000 Köln 90, West Germany

An experimental study was carried out on the effects of notch length, specimen thickness, ply thickness and type of defect (centre-notch or hole) on the fracture toughness of graphite–epoxy composites with lay-up sequences of 0/±45°/0 and 0/90°. Three fracture-mechanical concepts were applied: the Waddoups–Eisenmann–Kaminski (WEK) model, the Whitney–Nuismer model (point and average stress cirteria) and the K_R-curve method. An increase of notch length as well as an increase of ply thickness led to a higher toughness, whereas a change in specimen thickness did not noticeably affect the toughness. Furthermore, the hole caused a smaller strength reduction than a notch. The applicability of the above-mentioned concepts is probably restricted mainly because of the fact that they do not, or do only insufficiently, regard the damage zone near the border of the defect, if a large damage zone usually leads to larger material parameters of the investigated concepts, namely the inherent flaw size, the characteristic lengths of the point and average stress criterions and the K_R-value at fracture.

1. Introduction

In the study of fracture behaviour of composites, a great effort has been made [1–8] to explain the well-known phenomenon that larger holes (notches) cause greater fracture stress reductions than smaller holes (notches), a phenomenon which cannot be explained by a classical stress concentration factor. Many approaches have been proposed to characterize such a fracture behaviour, among which the Waddoups–Eisenmann–Kaminski (WEK) model [1], the point and average stress criteria model [4, 5] and the resistance (K_R curve, where K_R is the crack growth resistance) model [6–8] have been reported to provide a good description of the fracture behaviour of composites. The WEK model [1] assumes the existence of an intense energy (inherent flaw) region with a size of a^* which is modelled as a through-crack of constant length, extending perpendicular to the load direction. In the point and average stress criterions model, Whitney and Nuismer [4, 5] proposed a failure model based on the stress distribution near the notch tip, assuming that failure occurs when the stress over some distance d_0 in front of the notch tip is equal to or greater than the strength of unnotched material (point stress criterion) or when the average stress over some distance, a_0, equals the unnotched strength (average stress criterion). In these concepts, a^*, d_0 and a_0 are assumed to be material constants, independent of hole (notch) size. According to the crack-growth resistance, K_R-curve, model, in which the crack-opening displacement (COD)-deviation from linearity is assumed to be entirely the result of self-similar crack extension, the K_R-

*Present address: Department of Metallurgy, Kyoto University, Sakyo-ku, Kyoto 606, Japan.

0022–2461/82/082324–13$04.06/0

curve, the K_R value at unstable failure and the crack extension, Δc_f, at unstable failure are material constants, independent of hole (notch) size.

In this work, a^*, d_0, a_0, the K_R-curve, the K_R-value at failure and Δc_f were measured for various notch lengths, specimen thicknesses, single ply thickness and defect types (hole and centre-notch) using angle-ply graphite–epoxy composites. The results clearly showed the effects of notch length, specimen thickness, ply thickness and type of defect on the fracture behaviour of the present composites. This work further deals with the experimental determination of the extension of the damage zone at a notch tip and its relation to the fracture toughness of graphite–epoxy composites. Finally, the applicability of the WEK model, the point and average stress criteria model and the K_R-curve model, in view of the damage zone, is examined.

2. Materials and experimental procedure

The composite plates were prepared by DFVLR Braunschweig using a hot-press technique from T300/914C prepreg. The nominal single-ply thickness and fibre volume-fraction of the produced laminates were 0.125 mm and 0.60, respectively. Various types of lay-up sequences were used and are indicated in Table I. "0°" refers to the longitudinal direction, and "±45°" and "90°" refer to the respective inclinations from the "0°" direction. "s" means a symmetric repetition of sequence given in the parentheses. Samples CB-1, CB-3 and CB-5 are composed of 0° and ±45°, and Samples CB-2, CB-4 and CB-6 of 0° and 90° layers. Samples CB-1, CB-3 and CB-5 and Samples CB-2, CB-4 and CB-6, differ from each other in laminate thickness (1 or 2 mm) and/or single-ply thickness (0.125 or 0.25 mm). Effects of specimen (laminate) thickness were studied by comparing the results of Sample CB-1 with those of Sample CB-3 and the results of Sample CB-2 with those of sample CB-4; the effect of ply thickness were studied by comparing the results of Sample CB-5 with those of Sample CB-1 and CB-3, and the results of Sample CB-6 with those of Samples CB-2 and CB-4. The effect of notch length was investigated by using centre-notched specimens with a width, $W = 20$ and 40 mm, at a constant relative notch length, $2c_0/W = 0.50$, where c_0 is half the length of the original notch. The effects of specimen thickness and ply thickness were investigated by using centre-notched specimens with a width, $W = 20$ or 40 mm, and a relative notch length, $2c_0/W = 0.50$. The effect of the type of defect was measured on 20 mm wide specimens with a 6 mm hole or notch, respectively. The testing methods have been described in a previous paper [9]. Three specimens were used for each test and the results averaged.

3. Results and discussion

3.1. Ultimate tensile strength of unnotched specimens

The average ultimate tensile strenghts, σ_0, of three unnotched specimens for a width $W = 10$ mm for composite Samples CB-1 to CB-6 were 932, 920, 938, 928, 930 and 932 MPa, respectively. In spite of the difference of specimen thickness, ply thickness and stacking configuration, the values of σ_0 for each composite were nearly the same.

3.2. Effects of notch length, specimen thickness and ply thickness on stress–COD curves of centre-notched specimens

Fig. 1 depicts typical stress–COD curves of com-

TABLE I Sequence, specimen thickness and ply thickness of composites investigated in the present work

Sample number	Sequence*	Specimen thickness (mm)	Ply thickness (mm)
CB-1	$(0, +45°, -45°, 0_2, -45°, +45°, 0)$	1	0.125
CB-2	$(0, 90°, 0, 90°_2, 0, 90°, 0)$	1	0.125
CB-3	$(0, +45°, -45°, 0_2, -45°, +45°, 0)_s$	2	0.125
CB-4	$(0, 90°, 0, 90°_2, 0, 90°, 0)_s$	2	0.125
CB-5	$(0_2, +45°_2, -45°_2, 0_4, -45°_2, +45°_2, 0_2)$	2	0.250
CB-6	$(0_2, 90°_2, 0_2, 90°_4, 0_2, 90°_2, 0_2)$	2	0.250

*Each number stands for a prepreg layer. The figures 0, ± 45° and 90° without subscript refer to one momolayer of the prepreg and those with subscripts 2 and 4 refer to two and four layers of the prepreg, respectively. The subscript s means a symmetric repetition of the sequency given in the parentheses.

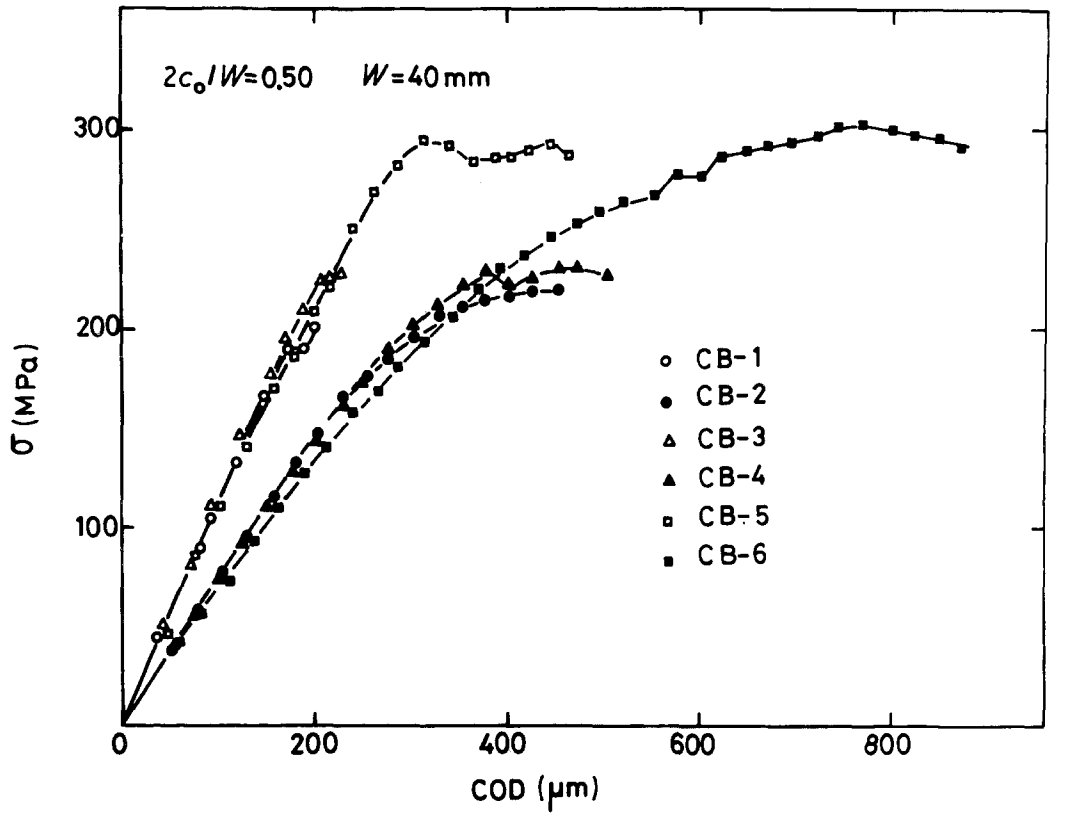

Figure 1 Gross stress–COD curves of Samples CB-1 to CB-6 composites with $W = 40$ mm and $2c_0/W = 0.50$.

posite Samples CB-1 to CB-6 for centre-notched specimens with $W = 40$ mm and $2c_0/W = 0.50$. If Sample CB-1 is compared with Sample CB-3, and if Sample CB-2 is compared with Sample CB-4, the shapes of the curves are nearly the same and the effect of the specimen thickness is not so large. On the other hand, comparison of Sample CB-5 with Samples CB-1 and CB-3, and comparison of Samples CB-6 with Samples CB-2 and CB-4 shows that the stress and COD at failure of the specimens composed of thicker plies are much larger than those of specimens composed of thinner plies. It is interesting to note that the COD values at fracture of the 0/±45°/0-type configurations (Samples CB-1, CB-3 and CB-5) were lower than those of the 0/90°-type configurations (Samples CB-2, CB-4 and CB-6).

3.3. Effects of notch length, specimen thickness and ply thickness on the stress intensity factor at fracture of centre-notched specimens

The finite-width correction factor for the present angle-ply laminate composites is different from the isotropic value. The difference is, however, less than a few per cent [10, 11]. Therefore, the infinite-width plate failure stress, σ_N^∞, was obtained for all laminates by multiplying the measured notched strength, σ_N, by the isotropic factor, Y, given by [12],

$$Y = [\sec(\pi c_0/W)]^{1/2}. \quad (1)$$

The stress intensity factor at failure, K_Q, was calculated from

$$K_Q = Y\sigma_N(\pi c_0)^{1/2}. \quad (2)$$

Fig. 2 shows the values of K_Q for various specimens. Three points are worth noting:

(a) If Sample CB-1 is compared with Sample CB-3 and if Sample CB-2 is compared with Sample CB-4, there is no large difference. This implies that the effect of specimen thickness on K_Q is very small.

(b) If Sample CB-5 is compared with CB-1 and CB-3, if Sample CB-6 is compared with Sample CB-2 and CB-4, there is a large difference. The thicker the ply, the larger is K_Q, although the values of σ_0 were nearly the same in all composites. A similar effect has been reported by Mandell *et al.* [13, 14], who found that, although

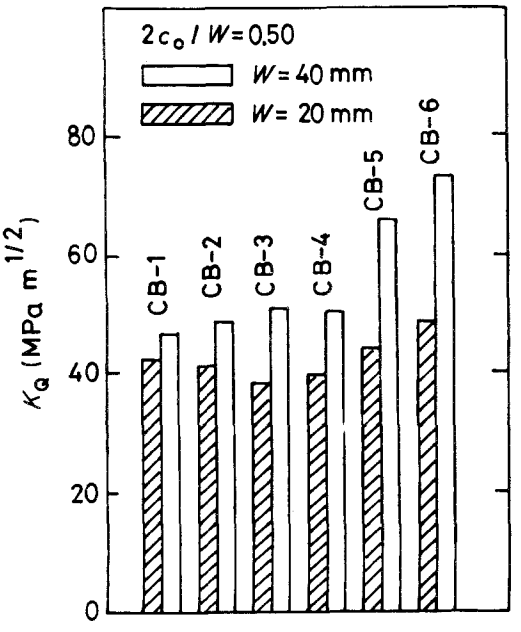

Figure 2 Measured values of K_Q of Samples CB-1 to CB-6 composites with $2c_0/W = 0.50$ and $W = 20$ or 40 mm.

the unnotched strength was relatively unchanged, the value of K_Q increased almost linearly with increasing ply thickness.

(c) On the specimens with larger notches, a higher toughness K_Q was reached in all cases.

3.4. Effects of notch length, specimen thickness and ply thickness on the inherent flaw size, a^*, and characteristic lengths, d_0 and a_0, of centre-notched specimens

In this section, effects of notch length, specimen thickness and ply thickness on the values of a^* of the WEK model and those on d_0 and a_0 of the point and average stress criteria are shown. As, in the case of centre-notched specimens, the inherent flaw size, a^*, of the WEK model is related to the characterisitc length a_0 of the average stress criterion by $a^* = a_0/2$ [15], only the characteristic lengths d_0 and a_0 will be considered in this section. According to the point and average stress criteria proposed by Whitney and Nuismer [4, 5], K_Q is given by

$$K_Q = \sigma_N (\pi c_0 \{1 - [c_0/(c_0 + d_0)]^2\})^{1/2} \quad (3)$$

for the point stress criterion and given by

$$K_Q = \sigma_N \left(\frac{\pi c_0 [1 - c_0/(c_0 + a_0)]}{1 + c_0/(c_0 + a_0)} \right)^{1/2} \quad (4)$$

for the average stress criterion. The characteristic lengths, d_0 and a_0, of each specimen were calculated by substituting the measured values of K_Q, σ_N and c_0, into Equations 3 and 4. The result is shown in Fig. 3. The values of d_0 and a_0 ($a_0 = 2a^*$) of the composites with thicker plies (Samples CB-5 and CB-6) are larger than those of the composites with thinner plies (Samples CB-1 to CB-4) for both 0/±45°/0 and 0/90° types. This feature is clearly found for the specimens with the larger width of $W = 40$ mm. Comparing Sample CB-1 with Sample CB-3, and CB-2 with Sample CB-4, it can be seen that the change of specimen thickness has little effect on d_0 and a_0. Another feature is that there is a large difference of d_0 and a_0 between specimens with different notch length for a given laminate. To summarize these results: the larger the notch and the thicker the ply, the larger the values of a^*, d_0 and a_0, while the specimen thickness has only a small effect on these values.

3.5. Effects of notch length, specimen thickness and ply thickness on K_R-curves and crack extension of centre-notched specimens

As the damage zone grows ahead of the crack tip, the load–COD curves deviate from linearity. Initial straight-line portions in the load–COD curves at various crack lengths were used to calculate the compliance. The compliance as a function of $2c_0/W$ was fitted to a polynominal by a least-square fit analysis, with the best-fit third degree polynominal. The effective crack length, by using this compliance calibration curve, was obtained for calculation of the crack growth resistance, K_R, at various load levels. K_R was calculated from

$$K_R = \sigma Y (\pi c)^{1/2}, \quad (5)$$

where σ and c are the nominal stress and effective half-crack lengths, respectively, and Y is the finite-width correction factor based on the effective crack length, given by $[\sec(\pi c/W)]^{1/2}$. According to the K_R-curve concept, the failure stress can be determined by the point of tangency between K_R in Equation 5 and the K-curve defined by $K = \sigma Y(\pi c)^{1/2}$ with σ as a parameter. For the 0/±45°/0-type laminates (Samples CB-1, CB-3 and CB-5), such a tangency point did not exist, as in our previous work [9]. Morris and Hahn [7] obtained the same result investigating $(0/\pm45°)_s$ and (0/90°/

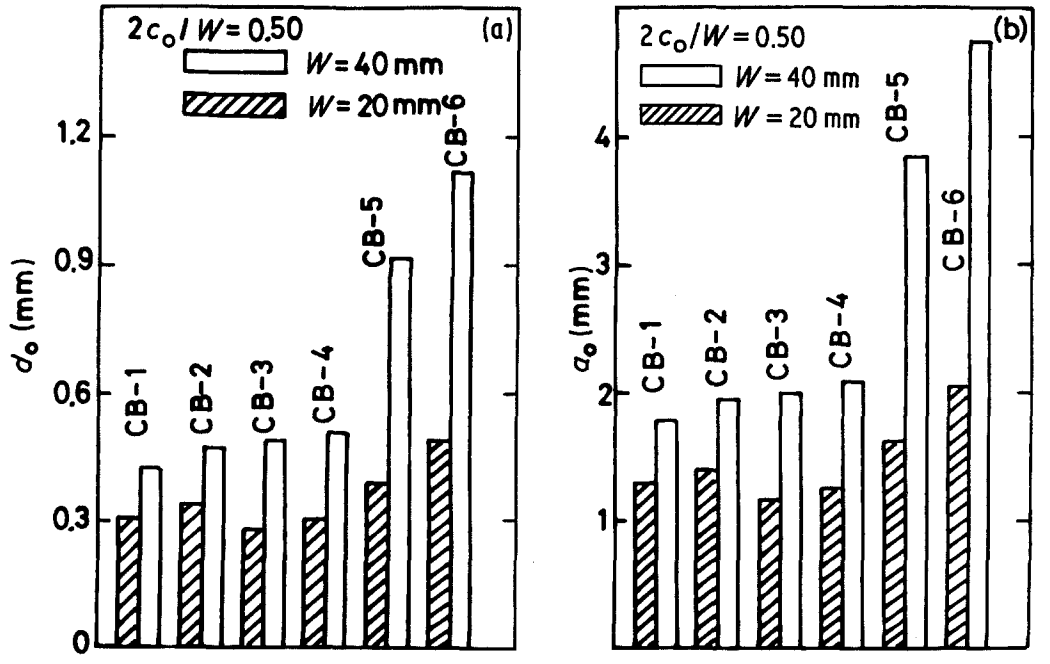

Figure 3 Calculated values of d_0 and a_0 of Samples CB-1 to CB-6 composites with $2c_0/W = 0.50$ and $W = 20$ or 40 mm.

$\pm 45^\circ)_s$ graphite–epoxy composites. For the $0/90^\circ$-type laminates, Samples CB-2 and CB-4, a tendency point was also not found, as shown in Fig. 4a and b. On the other hand, of the composite Sample CB-6, which showed the largest quasi-crack extension among the six composites investigated, one of the three specimens showed a tangency point, as shown in Fig. 4c. These results imply that, at least for the composite Samples CB-1 to CB-5, the K_R-curve cannot be used to predict a critical stress by the aid of a tangency point between K_R- and K-curves. For this reason the maximum value of K_R, namely K_R at failure, $K_{R,max}$ was taken for comparison. Also the quasi-crack extension, Δc_f, given by c_f-c_0, where c_f is the effective crack length at fracture, was measured from the K_R-c curves. The average values of Δc_f and $K_{R,max}$ for each composite are summarized in Fig. 5. The larger the notch and the thicker the ply, the larger the values of Δc_f and $K_{R,max}$, whereas a change of specimen thickness had little effect on either Δc_f or $K_{R,max}$.

The characteristic length, d_0, has been reported to be comparable with the quasi-crack extension at fracture, Δc_f, [7, 8], and from this finding it has been deduced that the K_R-curve method is reduced to the point stress criterion [8]. The present values of Δc_f in Fig. 5 are not comparable with the values of d_0 in Fig. 3 and the difference between Δc_f and d_0 seems to become larger with increasing fracture toughness. Therefore, Δc_f cannot be related, one to one, to d_0.

3.6. Effects of the type of defect (notch or hole) on fracture properties

In this experiment, the effect of a hole on the fracture toughness was investigated and compared with those of a centre-notch for the composite Samples CB-1 to CB-6. The experiment was carried out under the condition that both the radius of the hole, R, and half the crack length, c_0, were 3 mm at a specimen width of 20 mm resulting in $2R/W = 2c_0/W = 0.30$.

The value of the gross failure stress, σ_N^∞, was adjusted for all laminates by multiplying σ_N by the isotropic finite width correction factor for holes, given by [16],

$$\sigma_N^\infty = \sigma_N \frac{[2 + (1 - 2R/W)^3]}{3(1 - 2R/W)} \quad (6)$$

Assuming that linear elastic fracture mechanics and the inherent flaw concept [17], which were taken into consideration in the WEK model [1], are applicable to composite materials with a hole, the critical Mode I stress intensity factor, K_Q, for the unnotched specimen is given by

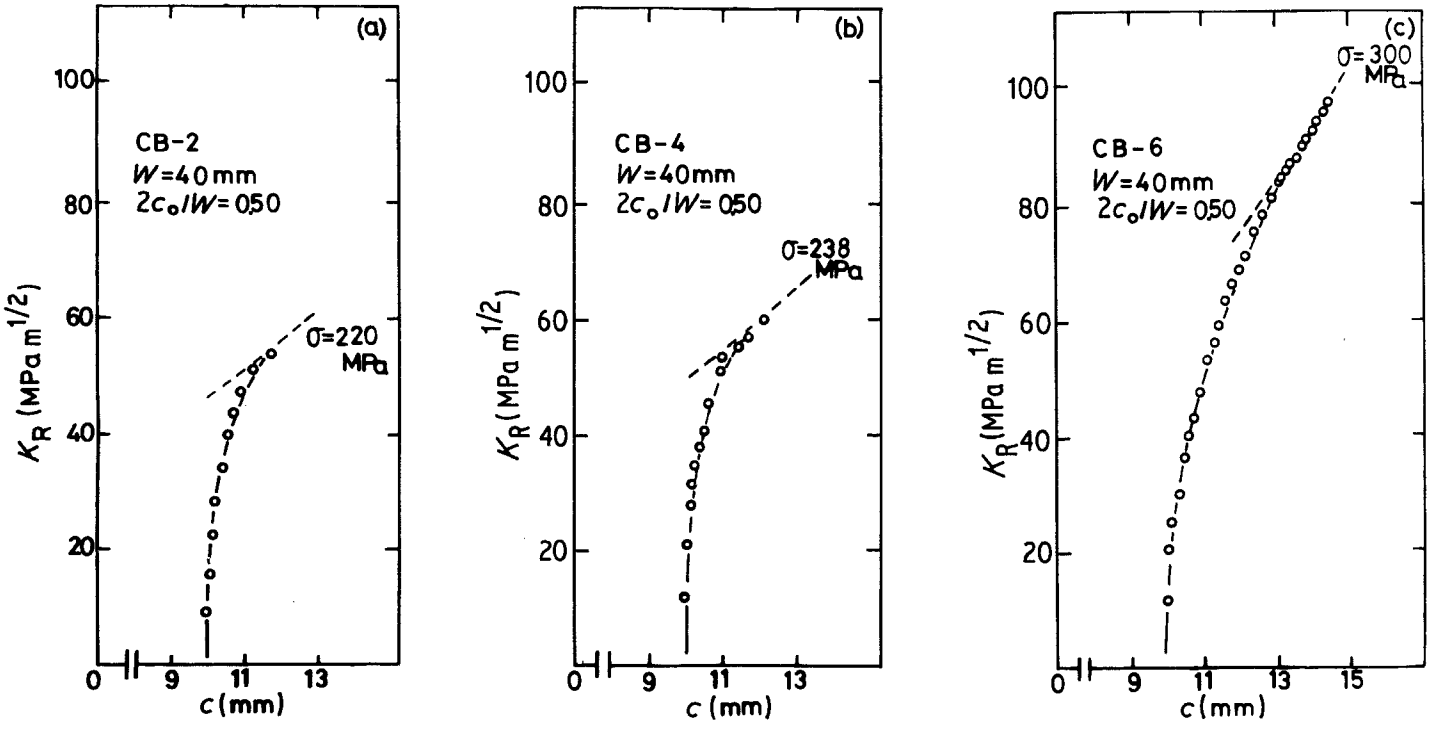

Figure 4 K_R-curves of Samples CB-2, CB-4 and CB-6 composites with $2c_0/W = 0.50$ and $W = 40$ mm.

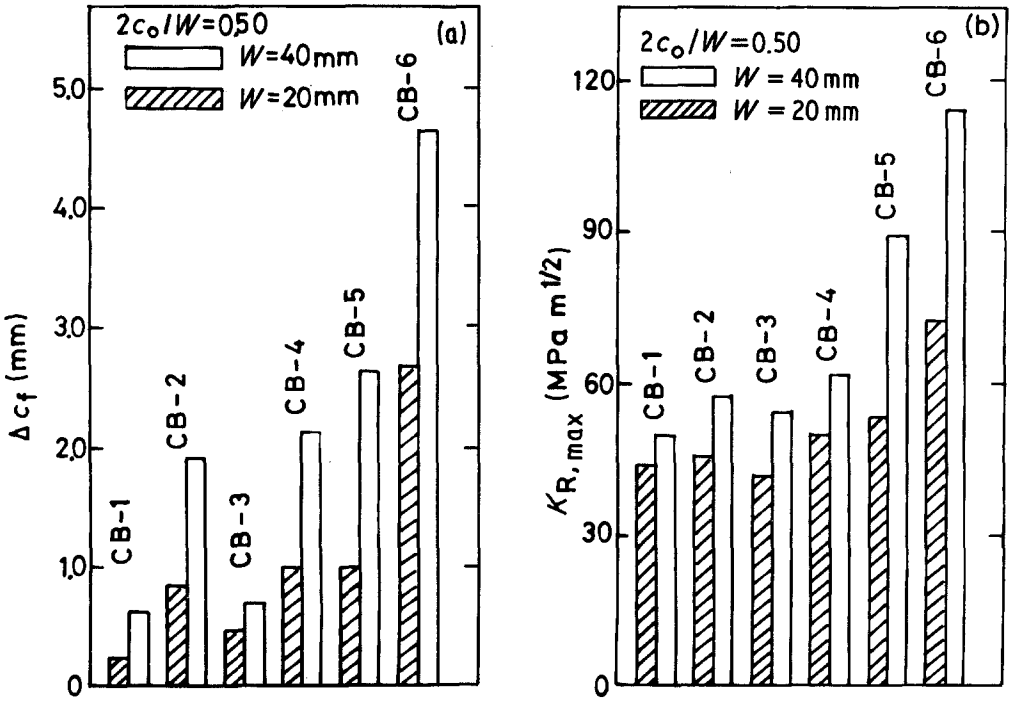

Figure 5 Measured values of Δc_f and $K_{R,max}$ for Samples CB-1 to CB-6 composites with $2c_0/W = 0.50$ and $W = 20$ or 40 mm.

$$K_Q = \sigma_0(\pi a^*)^{1/2}, \quad (7)$$

where a^* is, again, the length of the inherent flaw. For the specimen containing a hole with the inherent flaw, K_Q is given by

$$K_Q = \sigma_N^\infty(\pi a^*)^{1/2}F(a^*/R), \quad (8)$$

where $F(a^*/R)$ is a function given in [17]. Equating Equations 7 and 8 gives

$$F(a^*/R) = \sigma_0/\sigma_N^\infty. \quad (9)$$

Substituting the measured values of σ_N^∞/σ_0 into Equation 9, a^*/R and then a^* can then be determined. By substituting a^* back into either Equation 7 or 8, K_Q can be determined. The σ_N^∞/σ_0 and K_Q for Samples CB-1 to CB-6 with a hole are shown in Fig. 6, together with the results of the notched specimens. The values of σ_N^∞/σ_0 and K_Q for the specimens with a hole are between 10 and 30% and between 20 and 70%, respectively, higher than those for the notched specimens. Thus, it can be seen that the hole produces a smaller strength reduction than the notch.

According to the point and average stress criterions [4, 5], the ratio σ_N^∞/σ_0 for a hole is given by

$$\frac{\sigma_N^\infty}{\sigma_0} = \frac{2}{2+\xi_1^2+3\xi_1^4-(K_T^\infty-3)(5\xi_1^6-7\xi_1^8)} \quad (10)$$

for the point stress criterion and is given by

$$\frac{\sigma_N^\infty}{\sigma_0} = \frac{2(1-\xi_2)}{2-\xi_2^2-\xi_2^4+(K_T^\infty-3)(\xi_2^6-\xi_2^8)} \quad (11)$$

for the average stress criterion, where ξ_1 and ξ_2 are $R/(R+d_0)$ and $R/(R+a_0)$, respectively, and K_T^∞ is the orthotropic stress concentration factor for an infinitely wide plate. In the case of isotropy, $K_T^\infty = 3$, whereas, for anistropic materials the value of K_T^∞ deviates from 3 depending on the degree of anistropy. For the 0/±45°/0-type it can be assumed $K_T^\infty \approx 3$ [1, 18], whereas, for the 0/90°-type, $K_T^\infty = 5.11$ has been taken. The latter value was determined by Nuismer and Whitney [5] for a similar laminate, T300/5208. Substituting the measured values of σ_N^∞/σ_0 into Equations 10 and 11, the values of d_0 and a_0 can be determined for each composite. The values of d_0 and a_0 for notched specimens were determined from

$$\sigma_N^\infty/\sigma_0 = (1-[c_0/(c_0+d_0)]^2)^{1/2} \quad (12)$$

for the point stress criterion and were determined from

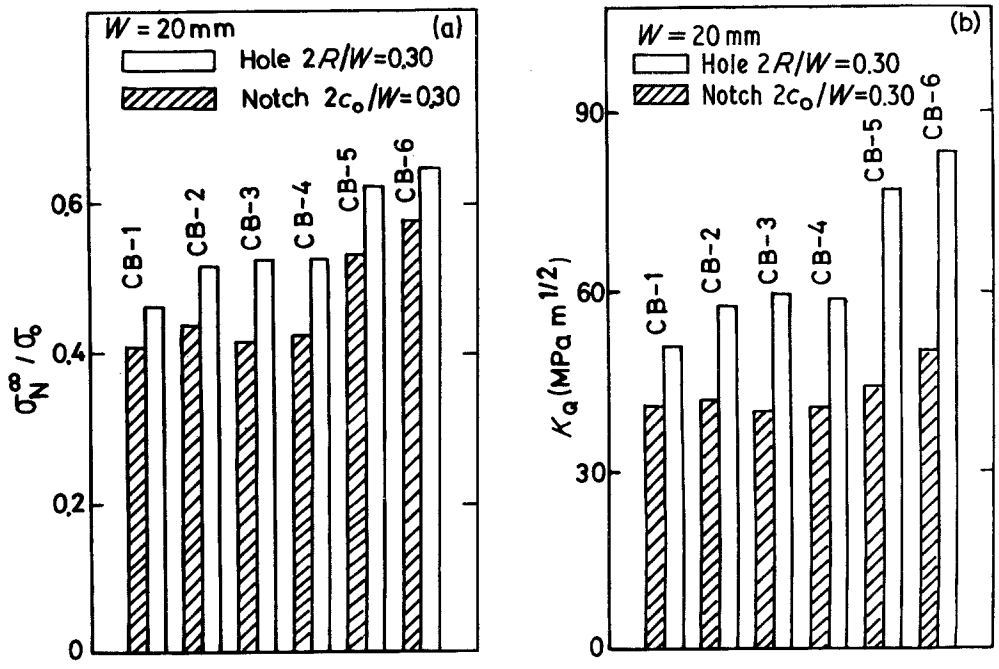

Figure 6 Measured and calculated values of $\sigma_N^{\infty}/\sigma_0$ and K_Q of Samples CB-1 to CB-6 composites with a hole of $2R/W = 0.30$ or a notch of $2c_0/W = 0.30$ at a constant $W = 20$ mm.

$$\sigma_N^{\infty}/\sigma_0 = \left(\frac{1 - c_0/(c_0 + a_0)}{1 + c_0/(c_0 + a_0)}\right)^{1/2} \quad (13)$$

for the average stress criterion. The results are presented in Fig. 7. Obviously, the characteristic lengths d_0 and a_0 of the specimens with a hole are much larger than those of the notched specimens. The calculated values of d_0, a^* and a_0 of each composite with a hole are indicated in Fig. 8. It is interesting to note that d_0 is approximately equal to $a^*/2$ for each composite, as pointed out by Prabhakaran [19] for his E-glass–epoxy composite.

The effect of specimen thickness and ply thickness on fracture properties was essentially the same, both for notched specimens and specimens with a hole, except that a hole resulted in a smaller strength reduction than a notch.

No model is available which satisfactorily describes the increasing toughness of specimens with larger notches and thicker plies. It may be reasonable to assume that the high toughness is related to the large value of the damage zone, since the damage zone in composites has a similar effect on the stress distribution as a plastic zone in high-strength metals. Thus, the large values of the parameters $a^*, d_0, a_0, \Delta c_f, K_Q$ and K_{Rmax} for composites with large notches and thick plies may be explained by the large value of the damage zone. A first step to establish the effect of the damage zone on these parameters is to investigate the form and size of this zone.

3.7. The form and size of the damage zone

The specimens were loaded to some given stress levels and after unloading they were examined using X-ray analysis to monitor the damage zone growth. A tetrabromethane opaque was applied to enhance the flaw image. Fig. 9 shows the typical appearance of the damage zone. In the 0/±45°/0-type composites, longitudinal subcracks in the 0° layer (0° subcracks) and subcracks in the ±45° layer (45° subcracks) were found, whereas the 0/90°-type composites showed 0° and 90° subcracks. It is a common feature in all composites that many subcracks were found, not only directly at the notch tip, but also away from the tip. The complex appearances of the damage zone made it difficult to treat them in a quantitative manner. An attempt was made to quantify the damage by measuring the length of the 0°, 45° and 90° subcracks, l_0, l_{45} and l_{90}, respectively, shown in Figs 10 and 11. As the damage zone could be regarded as a plastic zone in metals, the measured values of l_0, l_{45} and l_{90} were plotted against K^2 in Figs 10 and 11. Six remarks can be made:

(a) At low load, composite Samples CB-1,

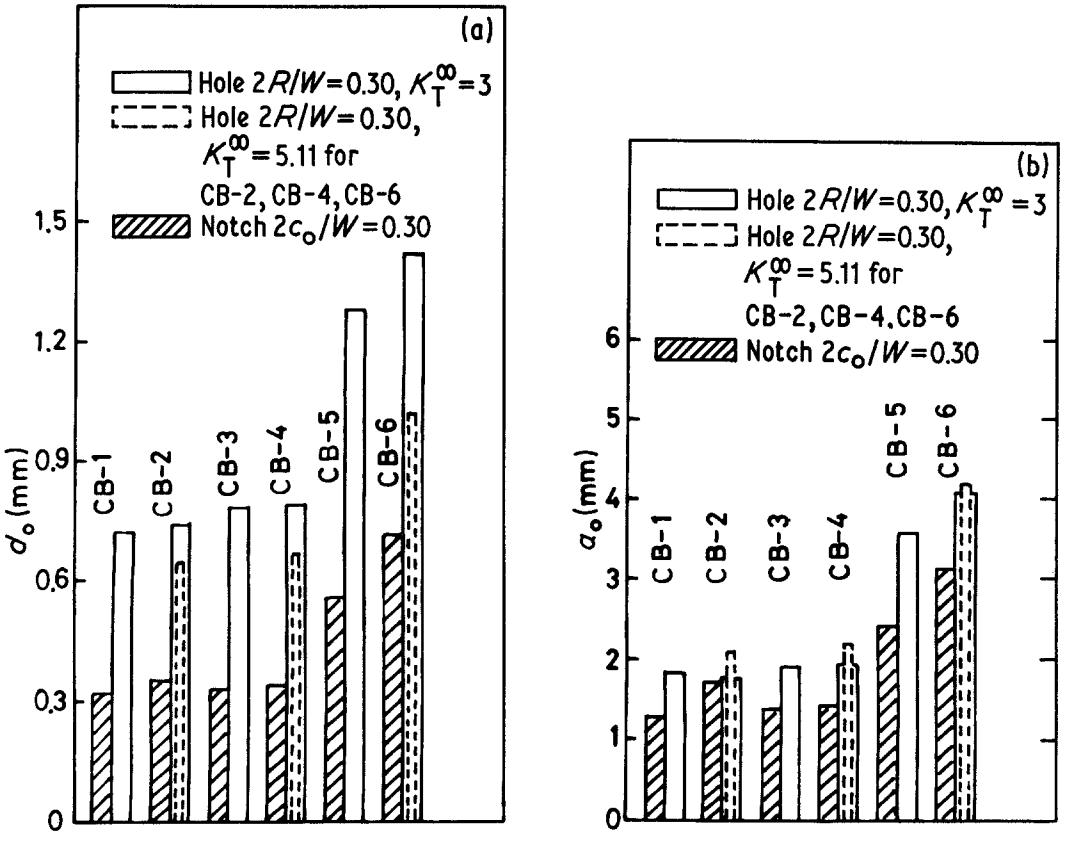

Figure 7 Calculated values of d_0 and a_0 of Samples CB-1 to CB-6 composites with a hole of $2R/W = 0.30$ or a notch of $2c_0/W = 0.30$ at a constant $W = 20$ mm. In the calculation, K_T^∞ was assumed to be 3 for Samples CB-1, CB-3 and CB-5, and it was assumed to be 3 and 5.11 for Samples CB-2, CB-4 and CB-6.

CB-3 and CB-5 with a 0/45°/0 configuration deformed elastically with no damage; no subcrack was observed up to some stress level, indicating the existence of a threshold stress at which subcracks form. On the other hand, in composite Samples CB-2, CB-4 and CB-6 with a 0/90° configuration, the subcracks formed at very low stress and they extend more rapidly than those in Samples CB-1, CB-3 and CB-5.

(b) The size of subcracks was not necessarily proportional to K^2.

(c) The results of Figs 10 and 11 show the tendency that, at the same stress intensity factor, K, the subcracks are longer when the single ply is thicker.

(d) Doubling the thickness of the laminate (compare Sample CB-1 with Sample CB-3, and Sample CB-2 with Sample CB-4) has been shown to have no visible effect on the subcrack lengths.

(e) The value of a_0 for the average stress criterion in Fig. 3 was smaller than the subcrack length measured by X-ray analysis. This is in contradiction to the results of Kim [8], who found that a_0 was comparable with the damage zone size, obtained from X-ray radiographs.

(f) It was impossible to correlate Δc_f with the size of subcracks in this work. However, in a qualitative manner, it was found, by comparing the size of subcracks in Figs 10 and 11 with Δc_f in Fig. 5, that the larger the subcrack length, the larger the value of Δc_f.

From the above results it is well understood that the large values of a^*, d_0, a_0, Δc_f, K_Q and $K_{R,max}$ are related to the large damage zone. The relationship between damage zone size and K_Q might be explained as follows: as the damage zone extends, the sharp notch is effectively blunted. Consequently, the stress at the notch tip is reduced, so that a higher stress must be applied to cause failure of the 0° fibres. The relationship between the damage zone size and a^*, d_0, a_0 and Δc_f will be discussed in Section 3.8. From this discussion, and from a consideration of the present data, a limit of applicability of the

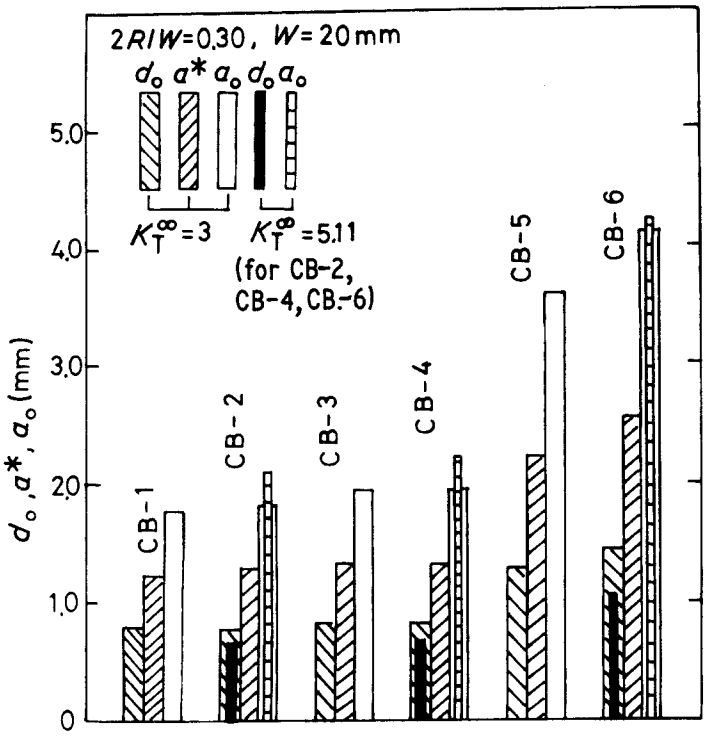

Figure 8 Comparison of d_0, a^* and a_0 of Samples CB-1 to CB-6 composites with a hole of $2R/W = 0.30$ and $W = 20$ mm. In the calculation for d_0 and a_0, K_T^∞ was assumed to be 3 for Samples CB-1, CB-3 and CB-5 and to be 3 and 5.11 for Samples CB-2, CB-4 and CB-6.

WEK model, point and average stress criterions model and K_R-curve model to the fracture behaviour of the present composites can be derived.

3.8. A limit of applicability of the WEK model, point and average stress criteria model and K_R-curve model to the fracture behaviour of graphite–epoxy composites

From the tests of varying the notch length, $2c_0$, at a constant relative notch length, $2c_0/W = 0.50$, and from the tests varying the type of defect (notch and hole), it was found that

(i) the larger the notch, the larger the a^*, d_0 and a_0 values (Fig. 3); and

(ii) specimens with a hole showed larger a^*, d_0 and a_0 values than notched specimens with the same notch size ($c_0 = R = 3$ mm).

These results suggest that a^*, d_0 and a_0 depend on the notch length and on the type of defect (notch or hole), although they are originally assumed as material constants in the WEK model and point and average stress criterions. Taking such a dependency into consideration, a modification of the WEK and the point and average stress criterions models is needed.

Concerning the K_R-curve model, it was shown that only in one case, at fracture of the specimen, was a tangency point found. This supports the suggestion that such a tangency point does not have a physical meaning, and that therefore, the fracture process cannot be predicted using the K_R-curve concept.

The difficulty is probably anchored in the damage zone, where the stress distribution is unknown. The stress distribution is not the same as for metals, where it can be assumed that in the plastic zone the stress does not exceed the yield stress and that the stress outside this zone can be described elastically, based on an effective crack length with the length of the physical crack plus half the plastic zone size. The damage zone in graphite–epoxy composites, however, causes the stress to lag behind the theoretical linear elastic stress distribution, and there is no constant stress at all in this zone because of the failing yield stress. For unidirectional B–Al it was found [20, 21] that the stress diminution at the notch tip is increasing at larger notch lengths, caused by the more-than-proportaional-to-K^2 extension of the plastic zone. The stress diminution of the notch tip causes the toughness to rise more than that suggested from the point and average stress criterions model. This means d_0 and a_0 are not material constants. In this study it was also found that d_0 and a_0, as well as a^* and Δc_f, depend on the notch length and on the type of defect. This is probably, again, the result of the influence of the damage zone.

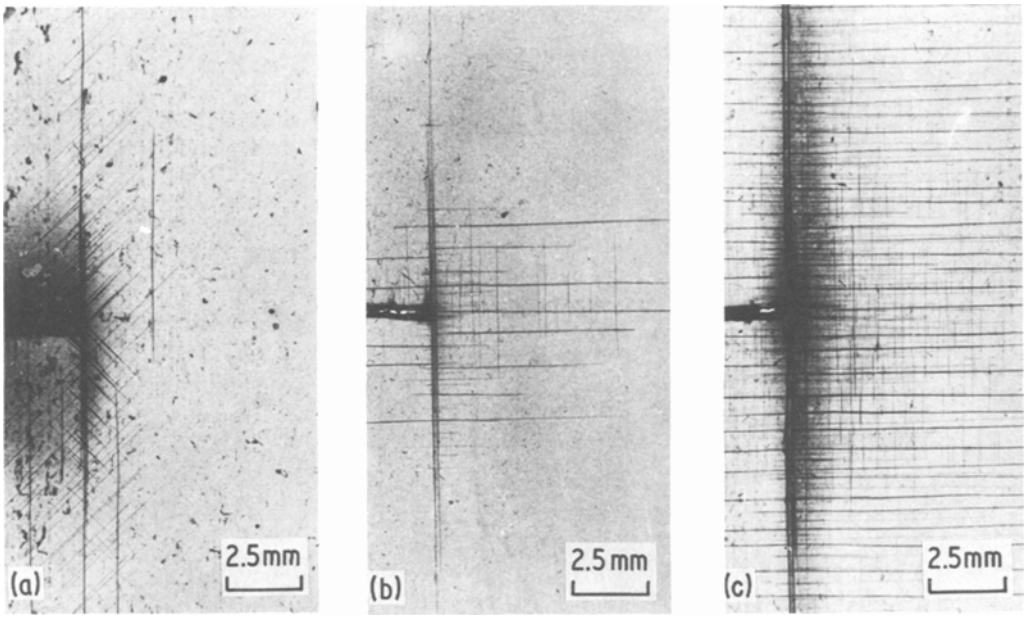

Figure 9 Appearance of the damage zone at (a) 75 % failure stress of Sample CB-5 and at (b) and (c), respectively, 65 % and 88 % failure stress of Sample CB-6, with $2c_0/W = 0.50$ and $W = 40$ mm.

Thus, the applicabilities of the WEK model, point and average stress criterions model and K_R-curve model may be limited. For these fracture-mechanical concepts, some modifications are needed, to take into consideration the effects of the configuration of the damage zone.

4. Conclusions

An experimental study was conducted on the fracture behaviour of graphite–epoxy laminates with a stacking sequence of the type $0/\pm45°/0$ or $0/90°$. The effect of notch length, specimen thickness, ply thickness and type of defect (notch and hole) on the fracture toughness was investigated, with emphasis on the extension of the damage zone. The applicabilities of the WEK model, point and average stress criterions model and K_R-curve model to the present composites was discussed. The main results obtained are as follows.

(a) The longer the notch and the thicker the single ply, the higher the fracture toughness. Accordingly, the inherent flaw size a^* in the WEK model , the characteristic lengths d_0 and a_0 in the point and average stress criterions models, and the effective crack extension, Δc_f, calculated from the compliance matching and K_R values at failure in the K_R-curve method all became larger. A change of thickness of the specimen (1 to 2 mm) had little effect on the above values.

(b) A hole in a specimen caused a smaller strength reduction than a notch of the same size. The stress intensity factor at fracture, the inherent flaw size a^* and the characteristic lengths d_0 and a_0 were larger in the case of specimens with a hole than in the case of specimens with a centre-notch.

(c) Observation of the damage zone using X-ray analysis showed that the size of subcracks along the fibre directions was not necessarily proportional to the square of the stress intensity factor. The notch length and defect shape dependence on the configuration of the damage is not sufficiently considered in the applied fracture mechanics concepts and the respective material parameters (a^*, d_0, a_0, Δc_f and K_R) are not material constant, as has been proposed in [1].

Acknowledgement

One of the authors (SO) wishes to express his gratitude to Professor W. Bunk for his invitation to his institute and to the Alexander von Humboldt Foundation for financial support of his stay in Germany.

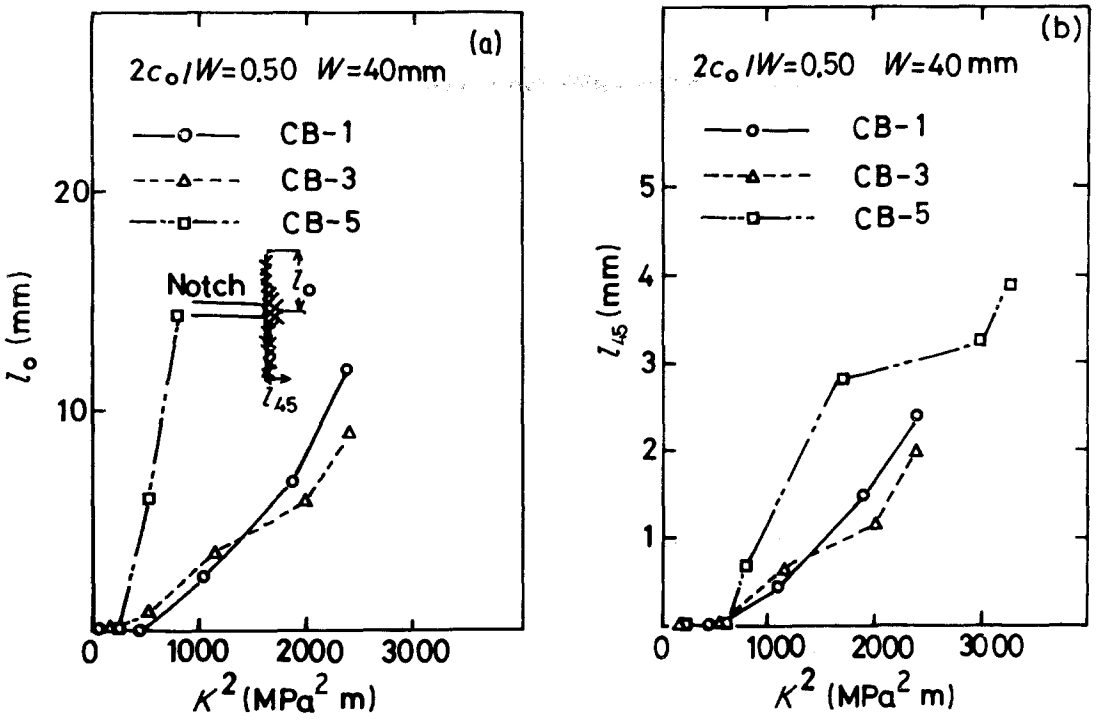

Figure 10 Measured values of l_0 and l_{45} of Samples CB-1, CB-3 and CB-5 with $2c_0/W = 0.50$ and $W = 40$ mm plotted against K^2.

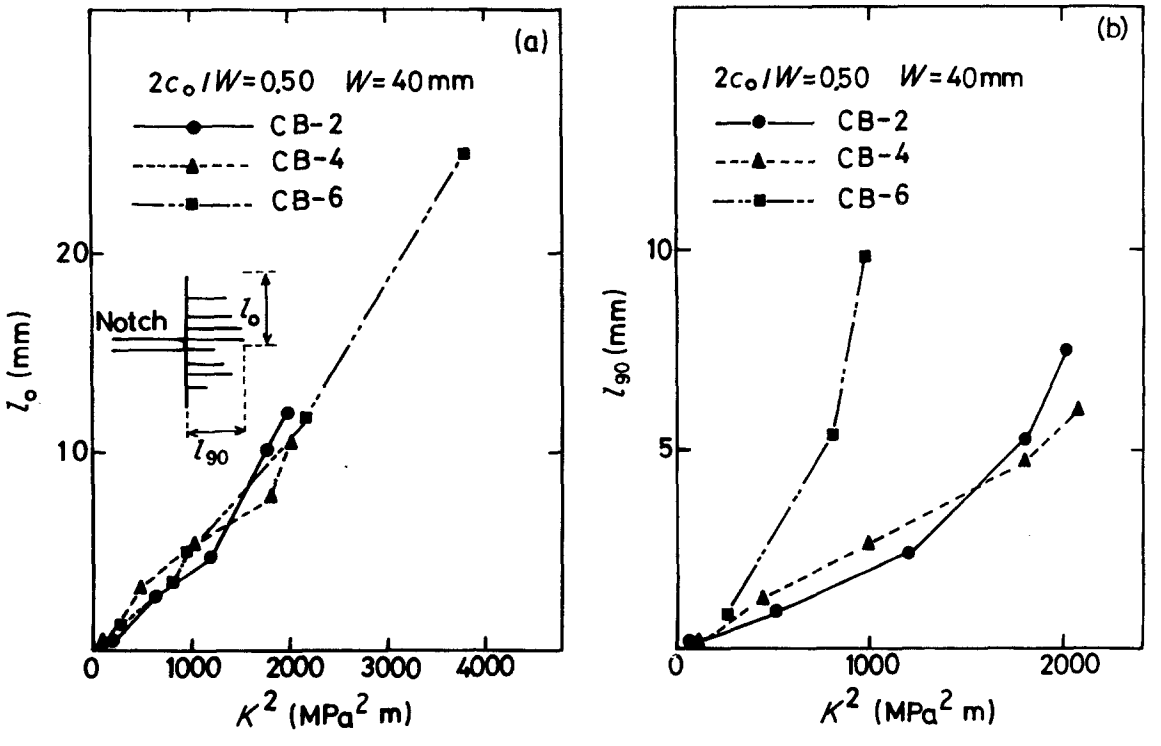

Figure 11 The measured values of l_0 and l_{90} of Samples CB-2, CB-4 and CB-6 composites with $2c_0/W = 0.50$ and $W = 40$ mm plotted against K^2.

References

1. M. E. WADDOUPS, J. R. EISENMANN and B. E. KAMINSKI, *J. Comp. Mater.* 5 (1971) 440.
2. J. C. HALPIN, K. L. JERINA and T. A. JOHNSON, "Analysis of the Test Methods for High Modulus Fibres and Composites" ASTM STP 521 (ASTM, Philadelphia, 1973) p. 5.
3. N. R. ADSIT and J. P. WASCZAK, "Fracture Mechanics of Composites" ASTM STP 593 (ASTM, Philadelphia, 1975) p. 163.
4. J. M. WHITNEY and R. J. NUISMER, *J. Comp. Mater.* 8 (1974) 253.
5. R. J. NUISMER and J. M. WHITNET, "Fracture Mechanics of Composites", ASTM STP 593 (ASTM, Philadelphia, 1975)p. 117.
6. S. GAGGAR and L. J. BROUTMAN, *J. Comp. Mater.* 9 (1975) 216.
7. D. H. MORRIS and H. T. HAHN, "Composite Materials", ASTM STP 617 (ASTM, Philadelphia, 1977) p. 5.
8. R. Y. KIM, *Exper. Mechan.* (2) (1979) 50.
9. S. OCHIAI and P. W. M. PETERS, *J. Mater. Sci.* 17 (1982) 417.
10. M. D. SYNDER and T. A. CRUSE, Air Force Materials Laboratory Technical Report number AFML-TR-73-209 (1973).
11. T. A. CRUSE and J. R. OSIAS, Air Force Materials Laboratory Technical Report number AFML-TR-74-111 (1974).
12. C. E. FEDDERSON, "Discussion" ASTM STP 410 (ASTM, Philadelphia, 1967) p. 77.
13. J. F. MANDELL, S. G. WANG and F. J. McGARRY, Air Force Materials Laboratory Technical Report number AFML-TR-74-167 (1974).
14. J. F. MANDELL, S. S. WANG and F. J. McGARRY, *J. Comp. Mater.* 9 (1975) 266.
15. S. W. TSAI and H. T. HAHN, "Inelastic Behaviour of Composite Materials" AMD, Vol. 13 (ASME, New York, 1975) p. 73.
16. P. C. PARIS and G. C. SIH, "Fracture Toughness Testing and Its Application" ASTM STP 381 (ASTM, Philiadelphia, 1965) p. 84.
17. O. L. BOWIE, *J. Math. and Phys.* 35 (1956) 60.
18. G. CAPRINO, J. C. HALPIN and L. NICOLAS, *Composites* (1979) 233.
19. R. PRABHAKARAN, *Mater. Sci. Eng.* 41 (1979) 121.
20. P. W. M. PETERS, Proceedings of the International Conference on Composite Materials III, Paris, 1980 (Pergamon Press, Oxford, 1980) p. 1153.
21. P. W. M. PETERS, PhD thesis, RWTH, Aachen (1981).

Received 30 November
and accepted 15 December 1981